



**HAL**  
open science

# Dynamic light scattering for the determination of linoleic acid critical micelle concentration. Effect of pH, ionic strength, and ethanol

Laure Degrand, Rebeca Garcia, Kevin Crouvisier Urion, Wafa Guiga

► **To cite this version:**

Laure Degrand, Rebeca Garcia, Kevin Crouvisier Urion, Wafa Guiga. Dynamic light scattering for the determination of linoleic acid critical micelle concentration. Effect of pH, ionic strength, and ethanol. Journal of Molecular Liquids, 2023, 388, pp.122670. 10.1016/j.molliq.2023.122670 . hal-04180238

**HAL Id: hal-04180238**

**<https://cnam.hal.science/hal-04180238>**

Submitted on 11 Aug 2023

**HAL** is a multi-disciplinary open access archive for the deposit and dissemination of scientific research documents, whether they are published or not. The documents may come from teaching and research institutions in France or abroad, or from public or private research centers.

L'archive ouverte pluridisciplinaire **HAL**, est destinée au dépôt et à la diffusion de documents scientifiques de niveau recherche, publiés ou non, émanant des établissements d'enseignement et de recherche français ou étrangers, des laboratoires publics ou privés.

# Journal Pre-proof

Dynamic light scattering for the determination of linoleic acid critical micelle concentration. Effect of pH, ionic strength, and ethanol

Laure Degrand, Rebeca Garcia, Kevin Crouvisier Urion and Wafa Guiga

PII: S0167-7322(23)01474-5  
DOI: <https://doi.org/10.1016/j.molliq.2023.122670>  
Reference: MOLLIQ 122670

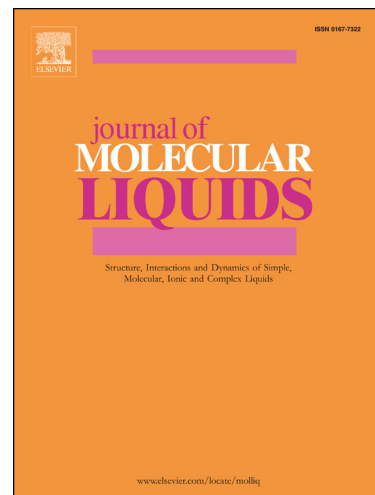
To appear in: *Journal of Molecular Liquids*

Received date: 9 March 2023  
Revised date: 21 July 2023  
Accepted date: 24 July 2023

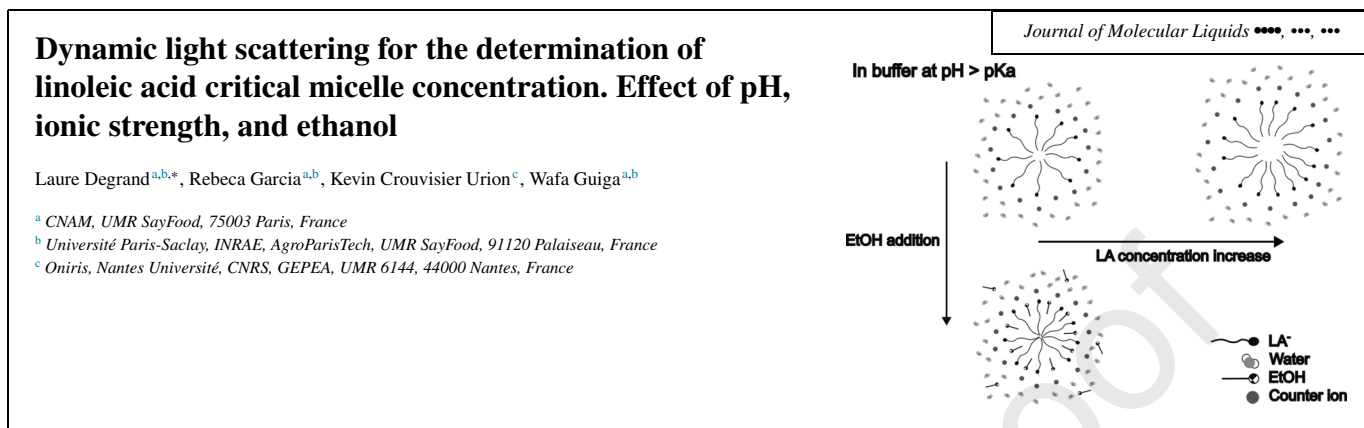
Please cite this article as: L. Degrand, R. Garcia, K. Crouvisier Urion et al., Dynamic light scattering for the determination of linoleic acid critical micelle concentration. Effect of pH, ionic strength, and ethanol, *Journal of Molecular Liquids*, 122670, doi: <https://doi.org/10.1016/j.molliq.2023.122670>.

This is a PDF file of an article that has undergone enhancements after acceptance, such as the addition of a cover page and metadata, and formatting for readability, but it is not yet the definitive version of record. This version will undergo additional copyediting, typesetting and review before it is published in its final form, but we are providing this version to give early visibility of the article. Please note that, during the production process, errors may be discovered which could affect the content, and all legal disclaimers that apply to the journal pertain.

© 2023 Published by Elsevier.



## Graphical abstract



### Highlights

- DLS is used to assess the value of CMC.
- DLS provides information on the dynamics of LA micelle formation in aqueous media.
- CMC is not affected by the addition of EtOH, increasing pH and Na<sup>+</sup> concentration.
- The decrease in size with the addition of EtOH leads to a better dispersibility.

Journal Pre-proof

# Dynamic light scattering for the determination of linoleic acid critical micelle concentration. Effect of pH, ionic strength, and ethanol

Laure Degrand<sup>a,b,\*</sup>, Rebeca Garcia<sup>a,b</sup>, Kevin Crouvisier Urion<sup>c</sup>, Wafa Guiga<sup>a,b</sup>

<sup>a</sup>*CNAM, UMR SayFood, 75003 Paris, France*

<sup>b</sup>*Université Paris-Saclay, INRAE, AgroParisTech, UMR SayFood, 91120 Palaiseau, France*

<sup>c</sup>*Oniris, Nantes Université, CNRS, GEPEA, UMR 6144, 44000 Nantes, France*

---

## Abstract

The present work proposes the use of Dynamic Light Scattering (DLS) to characterize aqueous solutions containing linoleic acid (LA). The parameters affecting CMC, particle size and distribution are studied. In a 0.2 M borate buffer, a CMC value of  $0.13 \pm 0.01$  mM was found, with particle size increasing from 200 to 800 nm with LA concentration. It appears that increasing the pH does not simply affect the CMC value but also modifies the stabilization of the particles. At pH 9, the medium is monodisperse and, at the highest LA concentrations studied, vesicle formation is suspected. At pH values around 10-11, the medium is polydisperse due to the dynamic equilibrium of micelle formation/disintegration. The counter ion concentration ( $\text{Na}^+$ ) has a significant effect on the particles size and number. The addition of ethanol also has an effect on the stability of the particles and leads to a decrease of the particle size without significantly affecting the CMC value.

*Keywords:* Linoleic acid, CMC, Dynamic Light Scattering, pH, ionic strength, ethanol

---

\*Corresponding author. E-mail address: laure.bertrand@lecnam.net

## 1. Introduction

Linoleic acid (LA) is an unsaturated fatty acid (C18:2), human essential, abundant in many vegetable oils. It is used in health care products, functional foods, pharmaceuticals, and cosmetics fields, especially because it is a precursor of physiologically active lipidic compounds with various effects on animals: hormone-like effect, inflammatory mediator or vasoconstrictor. It is widely studied in scientific research for its surfactant property. LA, as a poly-unsaturated fatty acid, is still a key platform molecule for chemical industry [1]. Historically and due to its physico-chemical properties, it was usually transformed by reactions in organic solvents. However, for reasons of sustainability, recent studies looked at transforming it using water or buffer as reaction media. Most studies focus on one of two approaches: either improving the performance of the catalysts (in particular enzymes as green catalysts, which requires genetic modification), or studying operation conditions of the process [2], [3], [4]. However, these studies often demonstrate a lack of knowledge about the structuring of the substrate (in this case LA) in these environments. The present study proposes a contribution to the understanding of the structuring of LA in aqueous media for the purpose of green solvent reaction.

Depending on pH and ionic strength, and for temperatures above the melting point of the hydrocarbon chain, fatty acids exist in different molecular species in relatively dilute aqueous solutions: un-ionized (neutral) fatty acids, acid-soap complex, carboxylate ions and ionic dimers [5]. In this article

we use the word soap according to its IUPAC definition [6], i.e. the salt form of the fatty acid in consideration. At room temperature, fatty acid molecules are not soluble in water. In these mixtures, at room temperature and above a certain concentration called the critical micellar concentration (CMC), long-chain fatty acid soaps can self-assemble into structures of various sizes [7] and shapes: rod-shaped or spherical micelles, or ellipsoidal vesicles [8]. This is because the hydrophobic group disrupts the hydrogen-bonded structure of water. To reduce the free energy of the system, surface-active molecules can aggregate into clusters with their hydrophobic groups directed towards the interior of the cluster and their hydrophilic groups directed towards the water. The structures of long-chain fatty acids clusters in excess of water have been summarized schematically as a function of pH and temperature [9].

The CMC value can be determined by any technique able of detecting a significant variation in the measured parameters related to the physico-chemical properties below and above CMC and, more particularly, to the monomeric or micellar state of the surfactants. Different methods can be used for this purpose: tensiometry [10], absorbance and fluorescence spectroscopy [11], conductimetry [12], etc. The main values recorded are presented Table 1 and it appears that most of them are determined by surface tension measurements [13], [14], [15], [16], [17], [18].

The ionic strength ( $I$ ) was calculated from equation (1) for each experimental condition listed in Table 1 according to the information given in the

Table 1: Main CMC values of LA reported in the literature

Ref	Measurement method or monitored parameter	Studied C range (mM)	Experimental conditions*			CMC (mM)	Est. I (mM)
			solvent/buffer	T	pH		
[13]	Surface tension (ST) <sup>(1)</sup>	0.005–0.130	0.2 M Tris buffer	NR	9.0	0.022	227
			0.2 M Tris buffer - 2% methanol	NR	9.0	0.025	-
			0.2 M Tris buffer - 5% methanol	NR	9.0	0.031	-
[14]	Surface tension <sup>(2)</sup>	0.020–0.400	0.5 M borate buffer	20 °C	9.0	0.150	120
[15]	Surface tension <sup>(2)</sup>	0.02–0.40	0.1 M sodium borate buffer	23 °C	10.0	0.167	236
			0.1 M sodium borate buffer	23 °C	9.0	gradual aggregation (0.06–0.32)	240
[16]	Surface tension <sup>(1)</sup>	0.750–5.500	NaOH	25 °C	11.2	1.700	3
			0.2 M trisodium phosphate buffer	25 °C	11.1–11.4	0.290	120
[17]	Surface tension <sup>(1)</sup>	0–0.600	0.5 M borate buffer - 5% ethanol	NR	9.0	0.225	120
[18]	Surface tension <sup>(1)</sup>	0.100–1.000	0.02 M phosphate buffer - 100 mM sodium formate or 100 mM NaCl	NR	10.4	0.240 or 0.230	-
			100 mM NaCl - 0.6% ethanol - 0.02 M phosphate buffer	NR	10.4	0.260	-
[19]	Initial radiolytic yield (G) <sup>(3)</sup>	0.100–0.250	NaOH	25 °C	9.0	2.000	0.3
[20]	Initial radiolytic yield <sup>(4)</sup>	0–2.000	little information of the exp. conditions	22 °C	9.0	2.300	-

\* Mentioned temperatures mostly correspond to the temperature of sample preparation;

C: LA concentration;

Est. I: estimated ionic strength;

NR: Not Reported;

<sup>(1)</sup> and <sup>(2)</sup>: CMC determined from the curves  $ST=f(C)$  or  $ST=f(\log C)$  respectively;

<sup>(3)</sup> and <sup>(4)</sup>: CMC determined from the curve  $G=f(C)$ . G is respectively calculated from the curve HPX concentration =  $f(\text{radiation dose})$  measured by UV absorbance spectrometry, or evaluated from oxygen uptake according to radiation dose.



literature. For some of them, the information is insufficient to make the calculation.

$$I = \frac{1}{2} \sum_i C_i z_i^2 \quad (1)$$

where  $C_i$  is the molar concentration of ion (M) and  $z_i$ , the charge of ion  $i$ .

Based on the Gibbs adsorption isotherm and provided that the ionic strength of the buffer is relatively high compared to the concentration of the surface-active agent, the CMC is obtained by plotting the measured surface tension versus the logarithm of the LA concentration. When the concentration is used directly instead of its logarithm, the results obtained are not easily interpretable. The two values shown in Table 1 corresponding to references [19] and [20] are determined indirectly by measuring the consumed  $O_2$  or the conjugated dienes formed after gamma irradiation. Other values obtained by conductimetry are questionable and are not reported in the table [21]. Indeed, electrochemical techniques cannot be applied due to the large number of ions present in the buffer.

The results presented in Table 1 show that pH influences the molecular species composition of LA in dilute aqueous solutions. As an example, Verhaegen et al. [15] showed that, at pH 9.0, aggregation occurred progressively over a wide range of concentration (0.06 to 0.32 mM) and attributed this effect to pre-micellar aggregation into dimeric acid-soap or higher aggregates. Unlike at pH 10.0, it was therefore not possible to determine an accurate CMC

value at pH 9.0. Data presented in Table 1 also suggest that the nature and ionic strength ( $I$ ) of the buffer or aqueous diluent have a significant effect on the CMC value. For example, the CMC values obtained by Allen [13] with an ammonium counterion are significantly lower than those obtained by the others authors with a sodium counterion. According to Chevalier and Zemb [22], the counterions provided by the salt would screen the group repulsions and thus contribute to the stabilization of the aggregates.

It can be noticed that for weak ionic strengths [16], [19], corresponding to CMC values higher than the concentration of the counterion in the aqueous solution, the CMC values are ten times higher than for the highest ionic strengths. Finally, Table 1 also shows that the addition of ethanol or methanol slightly increases the CMC value of LA, which is in agreement with the theoretical predictions of Chevalier and Zemb [22] and the experimental results of Crouvisier Urion et al. [23]. Considering these results in the literature, the CMC value of LA in aqueous medium seems to depend on several parameters and is delicate to determine. Spectroscopic techniques are among the techniques suitable for the determination of CMC. Nevertheless, the results obtained by fluorescence spectroscopy, for example, are questionable because the measurement requires the addition of a fluorescent probe that interacts with LA and can disrupt the dynamics of micelle formation.

Among other techniques, Dynamic light scattering (DLS) is a direct means of determination of CMC but it has rarely been used for this purpose, although it is described by several authors as an ideal technique for

determining CMC values of micelles formed in dilute solutions [11], [24]. When coherent, monochromatic light passes through a solution containing particles or droplets, depending on the optical parameters of the system, some of the light will be scattered. A sudden increase in the intensity of the scattered light associated with a slight increase in monomer concentration has been attributed to the formation of micelles that scatter light more strongly than the species dissolved in the solution, such as free monomers or counterions. The concentration at which this abrupt change occurs is considered equivalent to the CMC value. In addition to determining the CMC, DLS has several advantages: it can detect very small particles (down to 0.1 nm) such as micelles [25] and estimate the polydispersity of a suspension and thus determine the particle size distribution. The present work proposes using DLS as a new technique to evaluate the CMC values of LA suspensions in different physico-chemical conditions. Although the CMC value of LA is interesting to functionalize the molecule in many applications (stability of emulsions and foams ...), the present work focuses on LA as a precursor of aromatic compounds [26] or compounds with biological activities [27], [28] obtained by its enzymatic oxidation. The effects of pH, ionic strength and ethanol addition on the structure of LA in aqueous solution are studied in the common ranges used for soybean lipoxygenase (LOX) reactions.

## 2. Material and methods

### 2.1. Chemicals

All chemicals are listed in Table 2.

Table 2: List of chemicals

Chemical	Reference or CAS number	Purity	Supplier
NaOH	480507	98%	Carlo Erba
Ethanol	1.11727.1000	96%	Merck
Borax	1330-43-4	99%	Sigma
Boric acid	B-6768	99%	Sigma
LA	10-1802-13	99%	Larodan

### 2.2. Preparation of LA aqueous micellar solutions

All dispersants were prepared in deionized water. Boric acid-borax buffers (0.2 M in terms of borate or 0.05 M in terms of sodium) at pH 9.0 were prepared according to Holmes [29]. Borate buffers at pH greater than 9 were prepared according to Gomori [30]. For the diluted buffer: the 0.2 M borate buffer at pH 9.0 previously prepared was diluted to one tenth. The sodium ions concentration and ionic strength were reduced from 80 and 160 mM to 8 and 16 mM respectively. The borate buffers at pH 10.3 and pH 11.8 have sodium ion concentrations of 100 and 70 mM respectively. Prior to sample preparation, all dispersants were filtered through 0.2  $\mu$ m polyethylene terephthalate (PET) filters. Aqueous micellar solutions at LA concentrations of 0.5 mM or 2 mM were prepared by slowly stirring the LA in a warm buffer (around 50 °C). Diluted solutions were prepared from these stock solutions (between 0 and 2 mM).

### 2.3. Dynamic light scattering (DLS)

#### 2.3.1. Theoretical aspects

DLS technique is commonly used to determine the size of particles in colloidal dispersions. It detects the time-dependent fluctuations in the scattering intensity due to the Brownian motion of the particles in solution, typically in the submicron range. This intensity  $\langle I(t) \rangle$  fluctuation is represented by a normalized second-order autocorrelation function,  $G$ , as follows:

$$G(\tau) = \langle I(t) \times I(t + \tau) \rangle \quad (2)$$

where  $t$  is the sampling time of the correlator and  $\tau$  the time step variation. For a large number of monodisperse particles, the correlation function can be modelled by an exponentially decaying function:

$$G(\tau) = A \times [1 + B \times e^{-2 \times \Gamma \times \tau}] \quad (3)$$

where  $A$  and  $B$  are two constants and  $\Gamma$  is the decay rate ( $\text{m}^2 \cdot \text{s}^{-1}$ ) and is expressed as follows:

$$\Gamma = D \times q^2 \quad (4)$$

where  $D$  is the translational diffusion coefficient of the particles ( $\text{m}^2 \cdot \text{s}^{-1}$ ) and  $q$  is the magnitude of scattering vector ( $\text{\AA}^{-1}$ ) and expressed as follows:

$$q = \frac{4 \times \pi \times n}{\lambda_0 \times \sin \frac{\theta}{2}} \quad (5)$$

where  $n$  is the refractive index of the dispersant,  $\lambda_0$  is the incident laser wavelength ( $\text{\AA}$ ) and  $\theta$  is the scattering angle of the light. Fitting the above equations gives the value of the translational diffusion coefficient  $D$  of the particles. Assuming that the particles are non-interacting and spherical, their sizes (m) in solution (the hydrodynamic diameter  $d_H$ ) can be determined using the Stokes-Einstein relation:

$$d_H = \frac{k \times T}{3 \times \pi \times \eta \times D} \quad (6)$$

where  $\eta$  is the dynamic viscosity of the solvent (Pa.s),  $T$  is the absolute temperature (K) and  $k$  is the Boltzmann constant ( $\text{m}^2 \cdot \text{kg} \cdot \text{s}^{-2} \cdot \text{K}^{-1}$ ).

### 2.3.2. Experimental conditions

All measurements are performed on a Malvern Zetasizer, Nano ZS (Malvern Instruments Limited, U.K.) equipped with a 4 mW He-Ne laser operating at a wavelength of 633 nm and an avalanche photodiode detector (APD). The scattered light is detected at an angle of  $173^\circ$ . Measurements were carried out in disposable polystyrene cells using the standard operating procedure of the Zetasizer software. Series of suspensions of different LA concentrations were prepared from the stock solutions. The samples were placed in the cells and allowed to equilibrate. The cells were first rinsed with the sample and then, to avoid air bubbles, filled by pouring the sample down the wall. A com-

puter running Zetasizer nano software attached to the instrument controlled the data acquisition and processing. Prior to analysis, the sample parameters were set to the Standard Operating Measurement. Measurements were carried out at a fixed vertical position of 4.65 mm from the bottom of the cell and at  $25 \pm 0.1$  °C (i.e. above the LA melting temperature of  $-11^{\circ}\text{C}$ ). The refractive index of the material (LA) and dispersant were set at 1.47 and 1.33 respectively. At the wavelength used for the measurement, the absorbance of the LA was assumed to be zero. The viscosity of the dispersant (hydro-ethanolic mixture) was calculated on the basis of the properties of pure water, pure ethanol and their mixtures according to Jones and Harris [31] and Kadlec et al. [32]. The effect of temperature on the viscosity of the dispersant was calculated using the Ben Lakhdhar model [33] The correlation functions and the number of photons per second without taking into account the laser power attenuation (derived count rate, expressed as kcps i.e.  $10^3$  counts per second) were collected for each sample. The size distribution in intensity was calculated by the software taking into account the sample parameters.

### 3. Results

#### 3.1. Effect of LA concentration in 0.2 M borate buffer on sample structuring

The aim of this first step is to study the behavior of LA and sodium linoleate molecules (from 0 to 2 mM) under common experimental conditions of enzymatic oxidation by LOX [23]. To obtain a pure 13-hydroperoxide, the

enzymatic oxidation of LA by soybean LOX is usually conducted in a buffered medium at an optimum pH of 9.0. The fraction of the ionized form of LA at the pH commonly chosen for LOX assays can be obtained from the speciation curve of LA based on its pKa value:

$$f_{LA} = \frac{1}{1 + 10^{pH-pKa}} \quad f_{L^-} = \frac{10^{pH-pKa}}{1 + 10^{pH-pKa}} \quad (7)$$

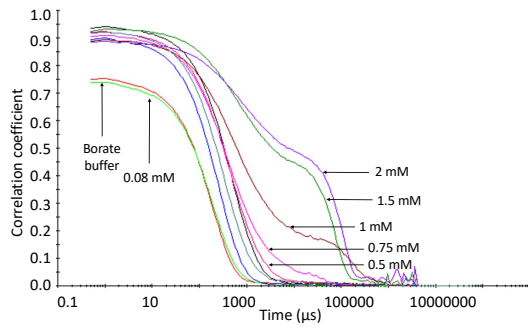
where LA is the protonated form of LA, L<sup>-</sup> its ionized form and f the molar fraction of the considered form. The pKa value of LA was determined experimentally at 7.9 by Bild et al. [34], which leads to 92,6% of the soap form at pH 9.0.

The obtained correlation functions (correlation coefficient versus time) at this pH (several examples are given in Figure 1-a) show that:

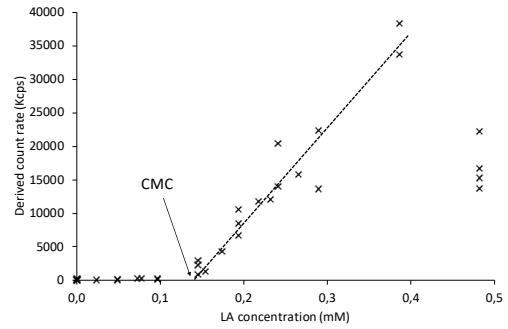
- from 0 to 0.5 mM LA, the decay line is steep, corresponding to a monodisperse sample, and extends with increasing particle size,
- from 0.5 mM to 2 mM LA, the decay line becomes softer as the LA concentration increases and shows breaks in slope relating to a poly-disperse sample.

The derived count rate is low (< 500 kcps) and stable from 0 to 0.1 mM of LA (Figure 1-b). This suggests the absence of a significant amount of light scattering particles. The derived count rate then increases rapidly between 0.1 and 0.4 mM of LA, reaching approximately 40,000 kcps. Knowing that the formation of micelles leads to the increase of the backscattering intensity, the

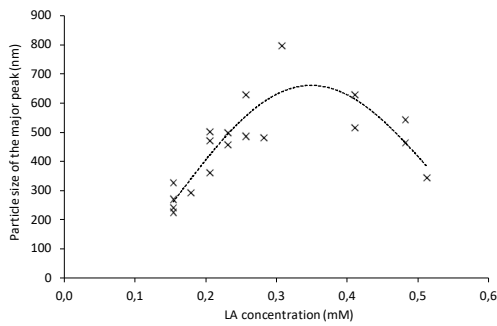




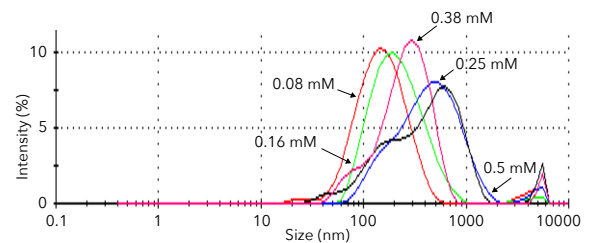
(a)



(b)



(c)



(d)

Figure 1: Correlation functions (a), derived count rate (b), size of the major peak in intensity (c) and an example of size distributions in intensity of LA dispersions in 0.2 M borate buffer at pH 9.0 as functions of LA concentration (d) - Correlation functions are plotted from intensity and equations (2) and (3), and size in intensity from equations (4) to (6).

disruption of the rate around 0.1 mM is therefore attributed to the CMC of LA under these experimental conditions. It is precisely determined at  $0.13 \pm 0.01$  mM, which is in agreement with the CMC value obtained in tensiometry by Lagocki et al. [14]. Verhagen et al. [15] did not observe a clear break in the slope with tensiometry measurements, due to the progressive formation of acid-soaps with the addition of LA. Linear interpolation of their results leads to an approximate CMC value of 0.138 mM.

Figure 1-d shows an example of the size distributions in intensity. The major peaks (peak area greater than 80% of the total peak area) of these size distributions are plotted against the LA concentration (Figure 1-c). For concentrations below the determined CMC value, no size can be calculated, logically due to the very low derived count rate, even though the size distribution curve shows a maximum percentage intensity at 150 nm. Indeed, as this distribution is presented as a percentage, the "major peak" does not correspond in this case to a significant light scattering intensity and is not validated as such by the software. For LA concentrations from 0.15 to 0.4 mM, the size of the major peak increases from 150 nm for the lowest concentrations to about 800 nm for the highest concentrations. From 0.5 mM, the correlation functions show high correlation coefficients even at times as long as several hundred milliseconds. This corresponds to high particle sizes ( $> 5 \mu\text{m}$ ) whose size cannot be correctly characterized by the Malvern software (data not shown). For further investigations, the LA concentrations studied do not exceed 0.5 mM.

These results are in agreement with the dynamics of the micelle formation presented by Patist et al. [35] for ionic surfactant. At concentrations below CMC, the lack of size distribution in intensity can be explained by the low formation of micelles due to low amounts of monomers and thus long intermolecular distance between monomers, limiting intermolecular interactions. At pH 9.0, a charged poly-ion results from the aggregation of the ionized form of LA. Oppositely charged counterions present in the solution (in this case  $\text{Na}^+$  ions) surround the negatively charged micelle. Their presence near the charged interface reduces its charge density and makes the aggregates stable by weakening electrostatic repulsions between head-groups. In addition, a slight 2% decrease in surface tension relative to water was observed and attributed to the high salt concentration of the buffer (See Table 3 in Supplementary Material). This effect is in favour of better micelle stability. Apel et al. [36] demonstrated that a stable hydrogen bonding network takes place between  $\text{COO}^-$  groups and  $\text{COOH}$  groups for pH close to pKa (acidic and ionic forms coexist) favoring the formation and stability of micelles and vesicles. Therefore, micelles can only grow by progressive incorporation of monomers [35]. This can be observed by the steady increase in size with increasing LA concentration from the CMC value (Figure 1-c). Some results in the literature, obtained by molecular dynamics simulations, show that LA or linoleate soaps form particles of hundreds of nanometers in diameter corresponding to lipid vesicles with clusters of solvent medium inside [37]. On this basis, it was hypothesized that, in this case, particles measured in size in

media of concentration above the CMC value probably correspond to vesicles. As more and more ionic surfactant is added to the system, the concentration of counterion surrounding these structures also increases, compressing the electrical double layer and reducing charge repulsion [35]. The particles move closer together so that attractive dispersion forces (i.e. van der Waals forces) lead to a reversible coagulation by fusion-fission mechanism.

### *3.2. Effect of pH in 0.2 M borate buffer on micelle formation*

Having studied the behavior of LA under the above conditions (commonly used in enzymatic lipoxygenation studies), the effect of pH change on micelle formation and consequently on the CMC value was investigated, in order to examine whether or not it is comparable to the results obtained for oleic acid by molecular simulation [37]. Solutions with a pH higher than 9 were prepared. The actual pH values were measured experimentally at 10.3 and 11.8.

Figure 2 shows that, compared to the values obtained at pH 9.0, the derived count rates recorded for pH 10.3 and 11.8 are very low in the studied LA concentration range. The values are about 100 kcps for LA concentrations below 0.2 mM and are erratic and below 1200 kcps for higher concentrations, especially at pH 11.8. At this pH, no CMC value can be determined in the range of LA concentrations studied. 99.99% of LA is in its ionized form suggesting nearly complete solubility and LA is present in its sodium soap form. At pH 10.3, the embedded figure in Figure 2 could be interpreted

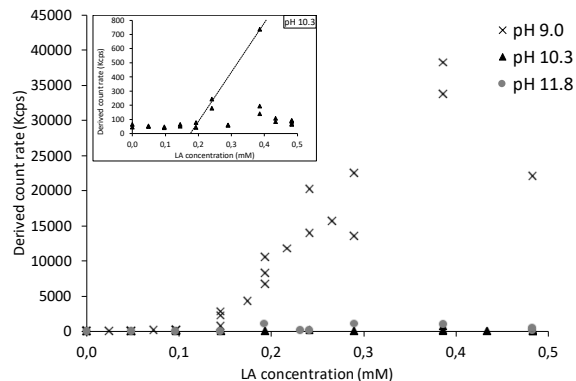


Figure 2: Derived count rate of LA dispersions in borate solution at different pH values as a function of LA concentration. The embedded figure shows a zoom of the pH 10.3 results.

as having a CMC value of about 0.178 mM, but the very low signal and poor data quality (derived count rate) make it difficult to assert this result. Verhagen et al. [15] observed in tensiometry that aggregation occurs over a wide range of LA concentrations for pH 9 (0.06 to 0.32 mM) while at pH 10 the CMC value was determined at 0.167 mM. In conclusion, based on this result obtained by Verhagen et al. [15], and considering our result as likely and relevant, the CMC of LA in borate buffer seems to be pH dependent.

The correlation functions for the experiments at pH 10.3 (see Supplementary Material, Figure 6) show low correlation between the signals (intercept of the correlation functions less than 0.85), which is in favor of a relatively high mobility of the detected particles (thus their small size) and their presence in small quantities in the medium. This suggests a high solubility of LA in its soap form and the formation of very small particles only within the

insoluble fraction. The size distribution in intensity shows two families of peak sizes: one at a few nanometers and one at a few hundred nanometers, with no apparent trend as a function of LA concentration.

By way of comparison, Janke et al. [37] demonstrated by molecular simulations that the total deprotonation of oleic acid ( $\text{pH} \gg \text{pKa}$ ) leads to the formation of micelles at low concentrations and vesicles of various shapes and sizes at high concentrations. They also demonstrated that the lower the pH (below pKa), the more regular the micelles obtained and the more stable they remain when the concentration increases. At  $\text{pH} > 9$ , LA micelles are in dynamic equilibrium, constantly disintegrating and reforming, resulting in populations of different sizes in the medium. Some results in the literature, obtained either experimentally (cryotransmission electron microscopy) or by molecular dynamics simulations, show that LA or linoleate soap form micelles of a few nanometers or less in diameter [19], [38]. The larger particles are therefore probably vesicles rather than micelles. This hypothesis deserves to be verified by Transmission electron microscopy (TEM) measurements that could be performed in future work.

In contrast to the borate buffer at pH 9.0, the higher pH borate solutions are inevitably composed of Borax supplemented with NaOH. Under the experimental conditions used in the present work, in addition to the change in pH, the concentration of the sodium cation and the ionic strength unavoidably undergo changes that may contribute to the change of the physical state of LA.

### 3.3. Effect of sodium ions concentration and ionic strength

In order to differentiate the effect of pH and the inevitably related effect of ionic strength and sodium concentration, two sets of experiments are performed. The first set consists in studying LA suspensions in a diluted borate buffer to decrease the  $\text{Na}^+$  concentration while maintaining the pH value at 9, the second set consists in modifying the sodium concentration by adding NaOH, thus modifying pH.

In the first set of experiments, the buffer dilution does not affect the pH, that remains constant. It affects the  $\text{Na}^+$  concentration and the ionic strength. As with the concentrated buffer (containing 80 mM  $\text{Na}^+$ ), the results obtained in the diluted buffer (containing 8 mM  $\text{Na}^+$ ) show a disruption in the change of the derived count rate related to LA concentration (Figure 3-b). This disruption corresponds to the formation of micelles. The CMC value is determined to be  $0.11 \pm 0.01$  mM under these conditions, and is not significantly different from the CMC determined in the undiluted buffer ( $0.13 \pm 0.01$  mM). Thus, we first conclude that at this pH, the change in  $\text{Na}^+$  concentration and ionic strength does not lead to a change in CMC.

However, the derived count rates in the diluted buffer are lower than in the concentrated buffer due to the formation of smaller and/or fewer micelles. Similarly, the correlation functions obtained for dispersions in the diluted buffer are characteristic of a monodisperse sample, except for the lowest LA concentration below the CMC value (Figure 3-a). The correlator sampling time is shorter than in the concentrated buffer (Figure 2) and the

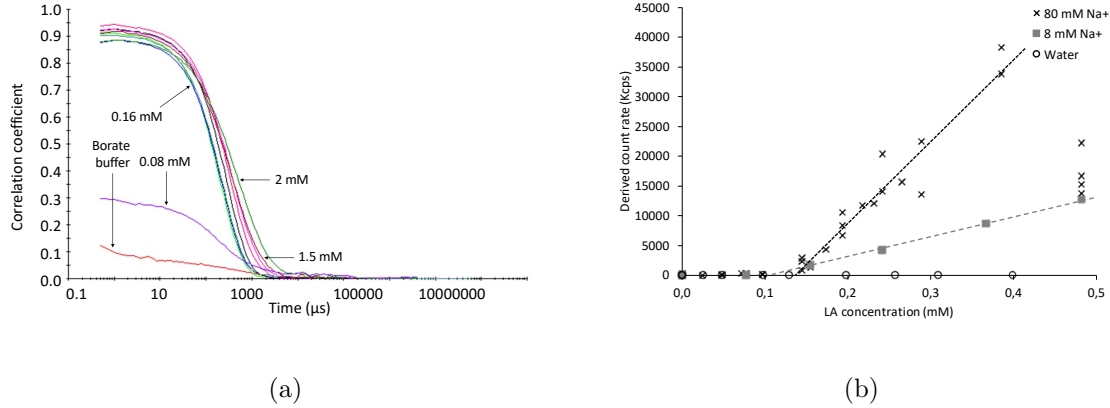


Figure 3: Correlation functions (a) and derived count rate (b) of LA dispersions in diluted borate buffer at pH 9.0 ( $[\text{Na}^+] = 8 \text{ mM}$ ) as functions of LA concentration - Correlation functions are plotted from intensity and equations (2) and (3).

correlation functions seem to depend on the LA concentration to a lesser extent in the concentration range studied (relatively constant steep decay). This observation would rather indicate the presence of smaller particles (than in undiluted media) of constant size, regardless LA concentration. The size distribution in intensity (See Figure 7 in Supplementary Material) shows a similar profile for each LA concentration ranging from 0.16 mM to 0.38 mM, with a major peak (over 95% of the total peak area) at  $165 \pm 3 \text{ nm}$ . This value is comparable to the particle size at the lowest concentration of LA at which micelles are detectable in concentrated buffer (Figure 1-c). The increase in derived count rate is then due to an increasing number of small micelles of the same size.

This is confirmed by the molecular dynamics simulation results obtained by Attia et al. [39]. The authors demonstrate that one sodium ion is able to



interact favorably with 2 or 3 carboxylate groups of linoleate; given the  $\text{Na}^+$ : linoleate ratio, it can be considered that there is no lack of sodium ions in all the experimental conditions tested in the present work, and that the addition of sodium does not improve the solubility of LA. The addition of large concentrations of counterions leads to the modification of their distribution in the bulk solution and around the aggregates: it reduces the structural charge of the aggregate by condensation of the counterion. The optimal micelle has an aggregation number and a charge such that its electrostatic surface energy is minimal [22]. Less added counterion leads to a smaller aggregation number and thus smaller micelle sizes.

The effect of the sodium ion concentration and ionic strength on the CMC value can therefore be considered insignificant in the range studied, in contrast to their effect on the micelle size distribution that increases with increasing  $\text{Na}^+$  concentration and ionic strength.

To investigate a wider range of  $\text{Na}^+$  concentrations and ionic strengths, including amounts corresponding to a lack of counterions, LA suspensions were studied in various concentrations of NaOH solutions (from 0.01 to 80 mM). At 40 and 80 mM NaOH, the pH is above 12. LA is in its ionized and completely soluble form. The derived count rate is stable and very low regardless LA concentration (results not shown). In this case, the effect of pH is largely dominating compared to the effect of sodium concentration. By comparison, the solubility of LA was found to be very low (CMC at 0.13 mM) in a borate buffer pH 9 with an excess sodium concentration of 80 mM.

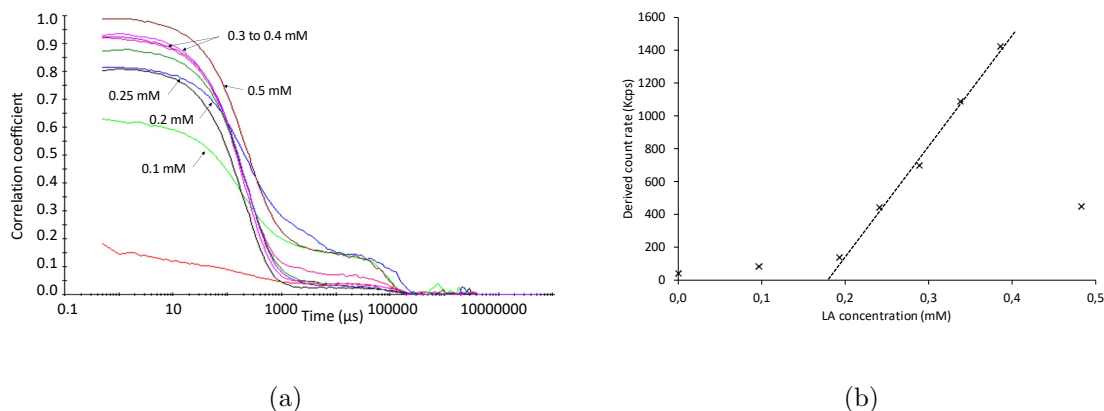


Figure 4: Correlation functions (a) and derived count rate (b) of LA dispersions in NaOH solution at 1 mM of ionic strength or sodium cation concentration (experimental pH 10.3) as functions of LA concentration - Correlation functions are plotted from intensity and equations (2) and (3).

We can thus conclude that the better solubility of LA at high pH values is not due to concentration of counter-ions but to the pH.

At 10 and 1mM NaOH, the pH was experimentally measured at 11.9 and 10.3 respectively. The low pH value at 1 mM NaOH (compared to the expected theoretical value of 11) is due to the partial dissolution of atmospheric carbon dioxide. At pH 11.9, LA is in its ionized form and 99.99% soluble. Correlation functions and size distribution curves are not relevant (data not shown), suggesting the absence of detectable particles. At pH 10.3 (1 mM NaOH), LA is in its ionized form at 99.6% and the correlation functions shown in Figure 4-a correspond to predominantly monodisperse samples.

As with the borate buffer assays, the evolution of the derived count rate as a function of LA concentration, shown in Figure 4-b, is divided in two

phases: at low LA concentration, the derived count rate is low and stable, then it increases with LA concentration. The CMC value can be determined at  $0.175 \pm 0.004$  mM for 1 mM NaOH (pH 10.3). This value is consistent with the value (0.167 mM) obtained by Verhagen et al. [15] and discussed above, and with the value of our present work presented in the previous section for borate solution at pH 10.3 (0.178 mM). This result confirms the prevalence of the effect of pH on CMC over the effect of  $\text{Na}^+$  concentration effect for pH values significantly higher than pKa. However, for comparable pH values, (e.g. 10.3), the borate medium leads to a higher dispersion of LA molecules than NaOH solution, as the former leads to samples with very low derived count rates (Figure 2 -  $< 800$  kcps). This can be explained by the concentration of sodium ions, which is ten times higher in the NaOH solution than in the borate buffer. In 1 mM of NaOH, the size distribution curve (Figure 8 in Supplementary Material) shows a major peak at a constant size of  $139 \pm 7$  nm in the LA concentration range studied, which is close to the particle size found in diluted borate buffer pH 9 (8 mM  $\text{Na}^+$ ).

In 0.01 mM of NaOH, the pH of the solution is below 8 and is not stable due to  $\text{CO}_2$  dissolution. Droplets on the surface of the LA suspension indicate the presence of LA in its acid form and a clear phase separation. The shape of the correlation functions, their intercept at  $t = 0$  s and the long sampling time of the correlator are in agreement with this experimental observation (results not shown).

In conclusion, we note that ionic strength and sodium concentration have

no significant effect on the CMC value but a significant effect on the size and number of micelles: LA dispersions in NaOH lead to predominantly monodisperse suspensions whereas in borate buffers a significant size distribution is noticed. Furthermore, at a similarly high pH ( $>10$ ), LA molecules tend to aggregate into smaller particles in the borate buffer than in NaOH solutions due to the lower sodium ion concentration.

#### 3.4. *Effect of ethanol concentration*

The literature data in Table 1 show a slight increase in CMC value in the presence of ethanol (0.6 to 5% v/v) or methanol (2 to 5% v/v). Furthermore, although they did not determine a CMC value, Crouvisier Urion et al. [23] recently hypothesized that a small amount of ethanol (2% v/v) improves the dispersibility or solubility of LA. However, the buffers used in previous studies (Tris buffer or 0.05 M borate buffer) to determine the CMC value do not correspond to the buffer commonly used for enzymatic lipoxygenation (borate buffer pH 9 or 10) and which is the focus of this work. Therefore, to study the effect of ethanol on LA micelles, two concentrations of ethanol (1 and 2% v/v) were added to borate buffer at pH 9.0. The effect of ethanol addition can be seen in the shape of the correlation functions (See Figure 9 in Supplementary Material). In the presence of ethanol, regardless the concentration (1 or 2% v/v), the correlation functions show a relatively constant steep decay. For the highest concentrations of LA, the presence of breaks in the slope corresponds to a bimodal sample. The shape of the curves presented in Figure 5 for LA

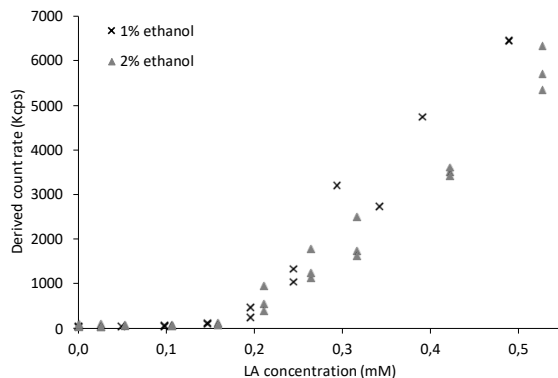


Figure 5: Derived count rates of LA dispersions in 0.2 M borate buffer at pH 9.0 (sodium concentration 80 mM) containing ethanol (1 or 2% v/v) as functions of LA concentration.

in the presence of buffer with added ethanol is similar to that obtained with LA in buffer alone (Figure 1-b).

The CMC value is determined at 0.18 mM for both concentrations of added ethanol. In agreement with the literature (reported in Table 1), this result shows that the addition of ethanol (1% v/v or 2% v/v) can only slightly increase the CMC value. The most noticeable effect is rather on the derived count rate values which are related to the particle size and/or number. Indeed, the size distributions in intensity (Figure 9 in Supplementary Material) show a major peak (over 90 % of the intensity area) of a relatively constant size (about 190 nm) for concentration values up to about 0.3 mM LA. Above this concentration, the sample is mainly a mixture of 100 and 500 nm micelles in the same proportions. The increase in the derived count rate is mainly due to the increase in the number of particles rather than their size. Compared to

the samples in buffer alone, at all LA concentrations below 0.5 mM, the particles are present at a smaller size (about 190 nm) corresponding to micelles. This result is in agreement with other works where stable hydrogen bonding is found between alcohols and carboxylate groups of fatty acids when the latter are mostly ionized (which is the case for all experimental conditions tested in the present work) [36], [40]. The addition of ethanol prevents the growth of micelles by progressive incorporation of the monomers, because the hydrogen bond between ethanol and carboxylate group is more stable than the hydrogen bond between two carboxylate groups.

This result is also in agreement with the results of surface tension measurements carried out on the different dispersants. The addition of ethanol had a decreasing effect on buffer surface tension: 7% for 1% EtOH and 9% for 2% EtOH (See Table 3 in Supplementary Material). This decrease was observed to a lesser extent by Phan [41] on a water/ethanol mixture. This difference can be attributed to the high salt concentration of the buffer mentioned above. The decrease in surface tension led to a lower interfacial tension and, hence, particle stabilization. Crouvisier Urion et al. [23] attributed their observation of enhanced activity of soybean LOX towards LA in the presence of 2% of ethanol, to greater dispersion - and therefore availability - of LA in the reaction medium thanks to ethanol.

#### 4. Conclusion

In the present work, the effect of several parameters on the formation of LA micelles and their size distribution was studied by DLS. The chosen technique proved to be ideal for this study, and its only limitation seems to be the delicate preparation of the sample to ensure the repeatability of the experiments. The well-known effect of pH was verified at pH values significantly above the pKa value of 7.9 of LA. At pH values  $\geq 11.8$ , LA is completely in its ionized form and no insoluble particles were detected in the conditions tested.

However, for lower pH values, pH does not seem to be the major parameter affecting the structuring of LA particles. Typically, in the commonly used borate buffer medium at pH 9 (92.6% in ionized form) for enzymatic reactions involving LA, the CMC was determined at 0.13 mM, the particle size increased from 150 to 800 nm with LA concentration and the mixture evolved from mono to polydisperse. Modification of  $\text{Na}^+$  concentration and ionic strength by borate buffer dilution had a significant effect on the size distribution of micelles, but the CMC value remained in the same range (0.11 and  $0.13 \pm 0.01$  mM). While in buffered media the micelle size distribution may be characteristic of polydisperse mixtures, the micelles were clearly monodisperse in 1 mM NaOH solution with a higher average size. Similarly, the addition of ethanol did not modify the CMC value but led to smaller particle size. Molecular dynamics simulations could be performed to study more precisely the effect of ethanol addition on LA self-assembly. Depending

on the desired applications, it is possible to either increase the solubility of LA in an aqueous medium (NaOH or high pH buffered medium), typically by increasing the pH of the buffered medium, or to modify the dispersibility of LA particles, typically by adding a small amount of alcohol. Furthermore, the possible presence of vesicles under certain conditions raises the question of the consequences on such heterogeneous reaction media, for example in terms of limiting the mass transfer of reactions. Their presence should thus be investigated by TEM in further research.

## References

- [1] U. Biermann, U. T. Bornscheuer, I. Feussner, M. A. R. Meier, J. O. Metzger, Fatty acids and their derivatives as renewable platform molecules for the chemical industry, *Angewandte Chemie International Edition* 60 (2021) 20144–20165. doi:<https://doi.org/10.1002/anie.202100778>.
- [2] A. Karout, C. Chopard, A. C. Pierre, Immobilization of a lipoxygenase in silica gels for application in aqueous media, *Journal of Molecular Catalysis B: Enzymatic* 44 (2007) 117–127. doi:<https://doi.org/10.1016/j.molcatb.2006.09.008>.
- [3] J. J. Villaverde, V. van der Vlist, S. A. Santos, T. Haarmann, K. Langfelder, M. Pirttimaa, A. Nyssölä, S. Jylhä, T. Tamminen, K. Kruus, L. de Graaff, C. P. Neto, M. M. Simões, M. Domingues, A. J. Silvestre, J. Eidner, J. Buchert, Hydroperoxide production from



- linoleic acid by heterologous *Gaeumannomyces graminis tritici* lipoxygenase: Optimization and scale-up, *Chemical Engineering Journal* 217 (2013) 82–90. doi:<https://doi.org/10.1016/j.cej.2012.11.090>.
- [4] C. Pang, S. Liu, G. Zhang, J. Zhou, G. Du, J. Li, Improving the catalytic efficiency of *Pseudomonas aeruginosa* lipoxygenase by semi-rational design, *Enzyme and Microbial Technology* 162 (2023) 110120. doi:<https://doi.org/10.1016/j.enzmictec.2022.110120>.
- [5] J. R. Kanicky, D. O. Shah, Effect of premicellar aggregation on the pKa of fatty acid soap solutions, *Langmuir* 19 (2003) 2034–2038. doi:<https://doi.org/10.1021/la020672y>.
- [6] D. H. Everett, Manual of symbols and terminology for physicochemical quantities and units, appendix ii: Definitions, terminology and symbols in colloid and surface chemistry, *Pure and Applied Chemistry* 31 (1972) 577–638. doi:[doi:10.1351/pac197231040577](https://doi.org/10.1351/pac197231040577).
- [7] A. J. Markvoort, N. Pflieger, R. Staffhorst, P. A. J. Hilbers, R. A. van Santen, J. A. Killian, B. de Kruijff, Self-reproduction of fatty acid vesicles: a combined experimental and simulation study, *Biophysical Journal* 99 (2010) 1520–1528. doi:<https://doi.org/10.1016/j.bpj.2010.06.057>.
- [8] D. M. Small, A classification of biologic lipids based upon their interac-

- tion in aqueous systems, *Journal of the American Oil Chemists' Society* 45 (1968) 108. doi:<https://doi.org/10.1007/BF02915334>.
- [9] D. P. Cistola, J. A. Hamilton, D. Jackson, D. M. Small, Ionization and phase behavior of fatty acids in water: application of the Gibbs phase rule, *Biochemistry* 27 (1988) 1881–1888. doi:<https://doi.org/10.1021/bi00406a013>.
- [10] N. S. Mousavi, S. Khosharay, Investigation on the interfacial behavior of aqueous solutions of cetyltrimethyl ammonium bromide in the presence of polyethylene glycols, *Fluid Phase Equilibria* 465 (2018) 58–64. doi:<https://doi.org/10.1016/j.fluid.2018.03.004>.
- [11] Ö. Topel, B. A. Çakır, L. Budama, N. Hoda, Determination of critical micelle concentration of polybutadiene-block-poly(ethyleneoxide) diblock copolymer by fluorescence spectroscopy and dynamic light scattering, *Journal of Molecular Liquids* 177 (2013) 40–43. doi:<https://doi.org/10.1016/j.molliq.2012.10.013>.
- [12] W. Al-Soufi, M. Novo, A surfactant concentration model for the systematic determination of the critical micellar concentration and the transition width, *Molecules* 26 (2021) 5339. doi:<https://doi.org/10.3390/molecules26175339>.
- [13] J. C. Allen, Soybean lipoxygenase, *European Journal of Biochemistry*

- 4 (1968) 201–208. doi:<https://doi.org/10.1111/j.1432-1033.1968.tb00194.x>.
- [14] J. W. Lagocki, E. A. Emken, J. H. Law, F. J. Kezdy, Kinetic analysis of the action of soybean lipoxygenase on linoleic acid, *Journal of Biological Chemistry* 251 (1976) 6001–6006. doi:[https://doi.org/10.1016/S0021-9258\(17\)33050-8](https://doi.org/10.1016/S0021-9258(17)33050-8).
- [15] J. Verhagen, J. F. G. Vliegthart, J. Boldingh, Micelle and acid-soap formation of linoleic acid and 13-L-hydroperoxylinoleic acid being substrates of lipoxygenase-1, *Chemistry and Physics of Lipids* 22 (1978) 255–259. doi:[https://doi.org/10.1016/0009-3084\(78\)90014-2](https://doi.org/10.1016/0009-3084(78)90014-2).
- [16] J. M. Gebicki, A. O. Allen, Relationship between critical micelle concentration and rate of radiolysis of aqueous sodium linoleate, *The Journal of Physical Chemistry* 73 (1969) 2443–2445. doi:<https://doi.org/10.1021/j100727a064>.
- [17] H. L. Tookey, R. G. Wilson, R. L. Lohmar, H. J. Dutton, Coupled oxidation of carotene and linoleate catalyzed by lipoxygenase, *Journal of Biological Chemistry* 230 (1958) 65–72. doi:[https://doi.org/10.1016/S0021-9258\(18\)70540-1](https://doi.org/10.1016/S0021-9258(18)70540-1).
- [18] M. W. Sutherland, J. M. Gebicki, A reaction between the superoxide free radical and lipid hydroperoxide in sodium linoleate micelles, *Archives*

- of Biochemistry and Biophysics 214 (1982) 1–11. doi:[https://doi.org/10.1016/0003-9861\(82\)90001-7](https://doi.org/10.1016/0003-9861(82)90001-7).
- [19] C. Hauville, S. Rémita, P. Thérond, A. Rouscilles, M. Couturier, D. Jore, M. Gardès-Albert, Determination of the yield of radiation-induced peroxidation of sodium linoleate in aqueous monomeric and micellar solutions, *Radiation Research* 150 (1998) 600–608. doi:<https://doi.org/10.2307/3579878>.
- [20] M. AlSheikhly, M. G. Simic, Chain-propagation length of linoleic acid peroxidation in aqueous monomeric and micellar systems, *The Journal of Physical Chemistry* 93 (1989) 3103–3106. doi:<https://doi.org/10.1021/j100345a045>.
- [21] M. B. Sierra, J. Rodríguez, R. M. Minardi, M. A. Morini, E. Aicart, E. Junquera, P. C. Schulz, The low concentration aggregation of sodium oleate-sodium linoleate aqueous mixtures, *Colloid and Polymer Science* 288 (2010) 631–641. doi:<https://doi.org/10.1007/s00396-009-2171-4>.
- [22] Y. Chevalier, T. Zemb, The structure of micelles and microemulsions, *Reports on Progress in Physics* 53 (1990) 279–371. doi:<https://doi.org/10.1088/0034-4885/53/3/002>.
- [23] K. Crouvisier Urion, R. Garcia, A. Boussard, L. Degrand, W. Guiga, Optimization of pure linoleic acid 13-HPX production by enzymatic re-

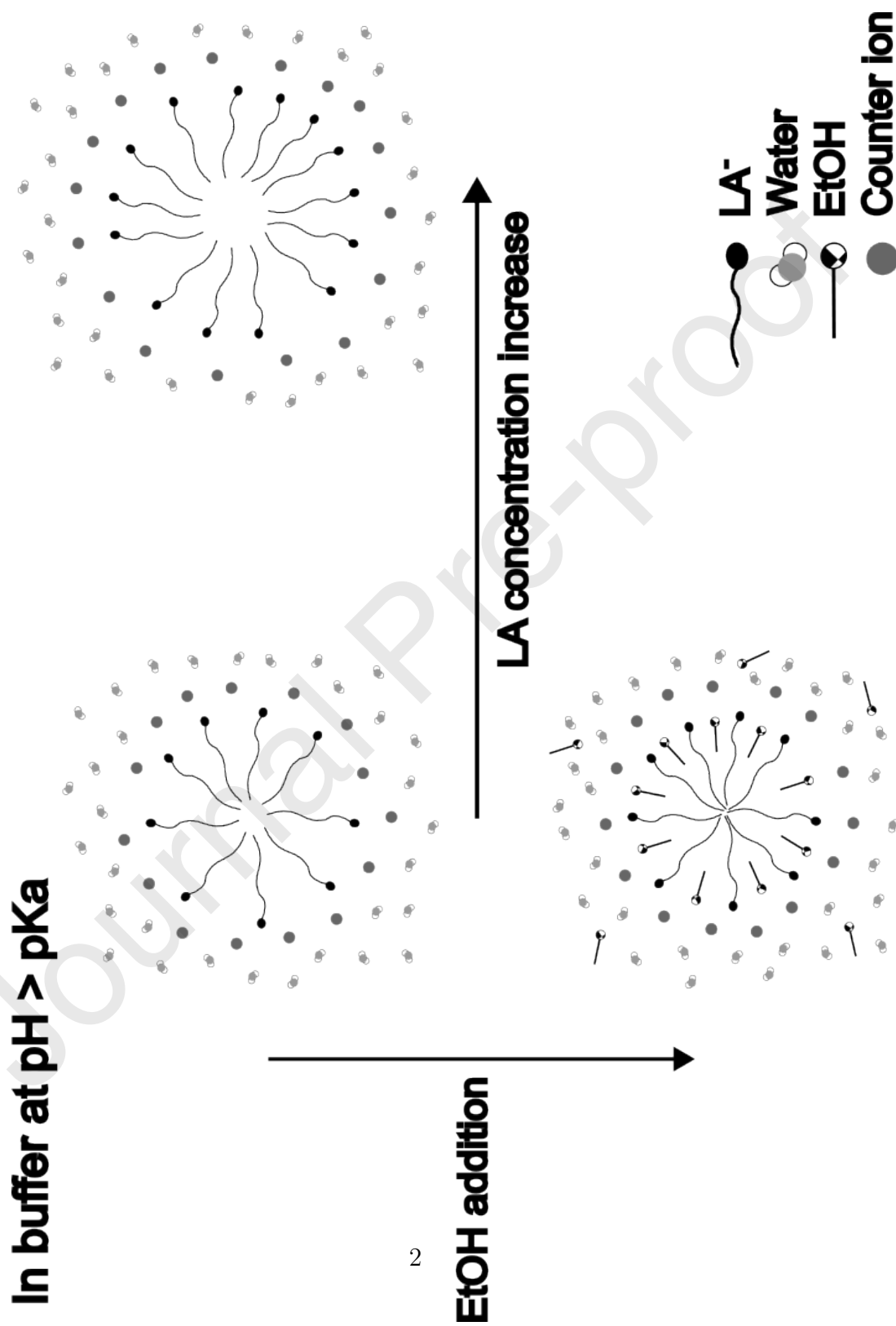
- action pathway: unravelling oxygen transfer role, *Chemical Engineering Journal* 430 (2022) 132978. doi:<https://doi.org/10.1016/j.cej.2021.132978>.
- [24] Malvern Instruments Ltd., 2010, Malvern application note: Surfactant micelle characterization using dynamic light scattering, URL: <https://www.malvernpanalytical.com/en/learn/knowledge-center/application-notes/an101104surfactantmicellecharacterization>.
- [25] Malvern Instruments Ltd., Livre blanc: a basic guide to particle characterization, Malvern Instruments Ltd., 2014.
- [26] M. Buchhaupt, J. C. Guder, M. M. W. Etschmann, J. Schrader, Synthesis of green note aroma compounds by biotransformation of fatty acids using yeast cells coexpressing lipoxygenase and hydroperoxide lyase, *Applied Microbiology and Biotechnology* 93 (2012) 159–168. doi:<https://doi.org/10.1007/s00253-011-3482-1>.
- [27] S. Matsushita, M. Kobayashi, Y. Nitta, Inactivation of enzymes by linoleic acid hydroperoxides and linoleic acid, *Agricultural and Biological Chemistry* 34 (1970) 817–824. doi:<https://doi.org/10.1271/bbb1961.34.817>.
- [28] M. Tsuchida, Y. Morishita, Antibacterial activity and bacterial degradation of linoleic acid hydroperoxide, *Bifidobacteria and Microflora* 14

- (1995) 67–74. URL: [https://doi.org/10.12938/bifidus1982.14.2\\\_67](https://doi.org/10.12938/bifidus1982.14.2\_67).
- [29] W. Holmes, Silver staining of nerve axons in paraffin sections, *The Anatomical Record* 86 (1943) 157–187. doi:<https://doi.org/10.1002/ar.1090860205>.
- [30] G. Gomori, Chap 16- Preparation of buffers for use in enzyme studies, in: *Methods in Enzymology*, volume 1 of *Methods in Enzymology*, Academic Press, 1955, pp. 138–146. doi:[https://doi.org/10.1016/0076-6879\(55\)01020-3](https://doi.org/10.1016/0076-6879(55)01020-3).
- [31] F. E. Jones, G. L. Harris, ITS-90 density of water formulation for volumetric standards calibration, *Journal of Research of the National Institute of Standards and Technology* 97 (1992) 335–340. doi:<https://doi.org/10.6028/jres.097.013>.
- [32] P. Kadlec, S. Henke, Z. Bubnik, Properties of ethanol and ethanol-water solutions – tables and equations, *Sugar Industry / Zuckerindustrie* 135 (2010) 607–613. doi:<https://doi.org/10.36961/si10420>.
- [33] M. Ben Lakhdar, Comportement thermohydraulique d’un fluide frigoporteur diphasique : le coulis de glace : étude théorique et expérimentale, PhD Thesis, INSA, Lyon, 1998.
- [34] G. S. Bild, C. S. Ramadoss, B. Axelrod, Effect of substrate polarity

- on the activity of soybean lipoxygenase isoenzymes, *Lipids* 12 (1977) 732–735. doi:<https://doi.org/10.1007/BF02570904>.
- [35] A. Patist, J. R. Kanicky, P. K. Shukla, D. O. Shah, Importance of micellar kinetics in relation to technological processes, *Journal of Colloid and Interface Science* 245 (2002) 1–15. doi:<https://doi.org/10.1006/jcis.2001.7955>.
- [36] C. L. Apel, D. W. Deamer, M. N. Mautner, Self-assembled vesicles of monocarboxylic acids and alcohols: conditions for stability and for the encapsulation of biopolymers, *Biochimica et Biophysica Acta (BBA) - Biomembranes* 1559 (2002) 1–9. doi:[https://doi.org/10.1016/S0005-2736\(01\)00400-X](https://doi.org/10.1016/S0005-2736(01)00400-X).
- [37] J. J. Janke, W. F. D. Bennett, D. P. Tieleman, Oleic acid phase behavior from molecular dynamics simulations, *Langmuir* 30 (2014) 10661–10667. doi:<https://doi.org/10.1021/la501962n>.
- [38] S. Abel, J. Attia, S. Rémita, M. Marchi, W. Urbach, M. Goldmann, Atomistic simulations of spontaneous formation and structural properties of linoleic acid micelles in water, *Chemical Physics Letters* 481 (2009) 124–129. doi:<https://doi.org/10.1016/j.cplett.2009.09.033>.
- [39] J. Attia, S. Rémita, S. Jonic, E. Lacaze, M. C. Fauré, E. Larquet, M. Goldmann, Radiation-induced synthesis and cryo-TEM characteri-

- zation of silver nanoshells on linoleate spherical micelles, *Langmuir* 23 (2007) 9523–9526. doi:<https://doi.org/10.1021/1a701366f>.
- [40] W. Xu, H. Zhang, S. Dong, J. Hao,  $^{133}\text{Cs}$  NMR and molecular dynamics simulation on bilayers of  $\text{Cs}^+$  ion binding to aggregates of fatty acid soap at high pH, *Langmuir* 30 (2014) 11567–11573. doi:<https://doi.org/10.1021/1a503193h>.
- [41] C. M. Phan, The surface tension and interfacial composition of water/ethanol mixture, *Journal of Molecular Liquids* 342 (2021) 117505. doi:<https://doi.org/10.1016/j.molliq.2021.117505>.





**Declaration of interests**

The authors declare that they have no known competing financial interests or personal relationships that could have appeared to influence the work reported in this paper.

The authors declare the following financial interests/personal relationships which may be considered as potential competing interests:

Journal Pre-proof

## **CRedit authorship contribution statement**

Manuscript “Dynamic light scattering for the determination of linoleic acid critical micelle concentration. Effect of pH, ionic strength, and ethanol”

**Laure Degrand:** Conceptualization, Validation, Methodology, Investigation, Formal analysis, Writing – Reviewing and Editing.

**Rebeca Garcia:** Writing – Reviewing.

**Kevin Crouvisier Urion:** Writing – Reviewing.

**Wafa Guiga:** Conceptualization, Validation, Methodology, Investigation, Formal analysis, Writing – Reviewing and Editing.

Journal Pre-proof